# UNSTEADY AERODYNAMIC HEATING OF A WINGED VEHICLE AND OPTIMUM REENTRY TRAJECTORY

JIRO KONDO

*Professor, Department of Aeronautics*
*University of Tokyo*

## ABSTRACT

The problem of the aerodynamic heating of a winged reentry vehicle is discussed from two sides. The unsteady temperature distribution over a thin wing is investigated in the first part of the paper and the optimum reentry trajectory of a winged vehicle for minimizing the total aerodynamic heating effect is studied in the second part.

## PART I

## INTRODUCTION

The fundamental system of equations for a laminar boundary layer of a compressible fluid consists of the conservation equations for mass, momentum, and energy, the equation of state and the equations describing the transport properties of air. The solution depends upon the boundary conditions on the surface of a body. The velocity is taken to be zero on the surface. For the temperature on the surface, on the other hand, either the adiabatic-wall assumption or the equitemperature-wall condition has usually been postulated simply for the convenience of analysis. No satisfactory foundations for these assumptions seem to be established. Figures 1*a*, *b* indicate the velocity and temperature profiles in the boundary layer of a flat plate at Mach 2 at several values of wall temperature. Since the boundary-layer solutions depend on the wall condition, it is worthwhile to determine the proper value of the wall temperature or the temperature distribution on the solid wall.

The wall temperature should be determined by solving the equation of heat conduction in the body which is under the influence of aerodynamic heating through the boundary layer. However, because the rate of aerodynamic heating depends on boundary-layer flow, the heating rate itself turns out to be dependent on the wall temperature. This means that the boundary layer around a body and the heat conduction in a body must be solved simultaneously.

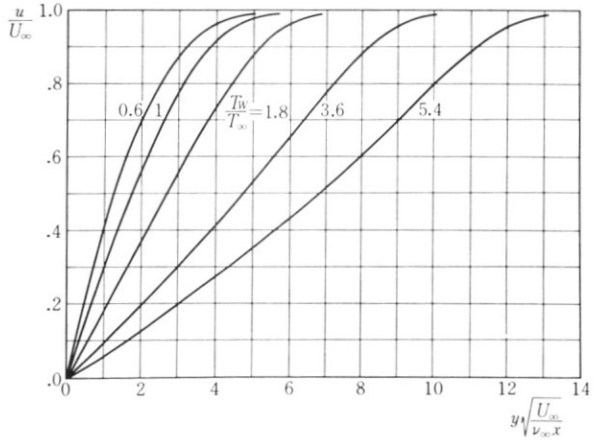


Figure 1*a*. Velocity profile in the boundary layer over a flat plate at various temperatures.

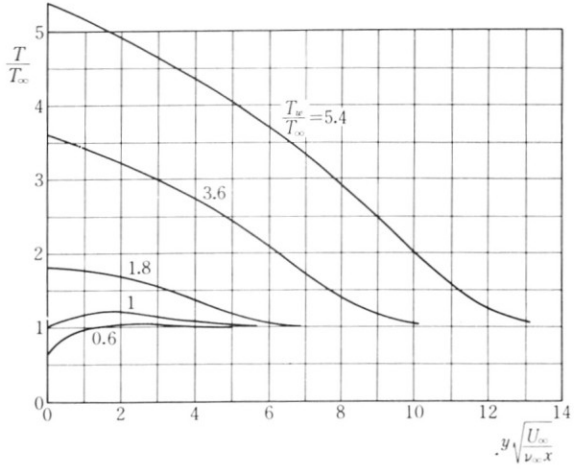


Figure 1*b*. Temperature profile in the boundary layer over a flat plate at various temperatures.

Although we are interested in the study of the unsteady temperature distribution of a body, we shall restrict ourselves to the case of quasi-steady heat transfer in the body and calculate the aerodynamic heating rate by means of a steady-state boundary-layer solution, since the equilibrium state in the velocity and temperature distribution is established very rapidly [1].

The problem will be reduced to that of determining the surface temperature by introducing the heat-transfer rate through the boundary layer on a wall with arbitrary temperature distribution in the equation of heat conduction. Emmons [2] solved the nonsteady aerodynamic heating of a plate utilizing the heat-transfer rate obtained by Chapman and Rubesin [3]. The solution is restricted to the case in which the surface temperature of a flat plate is expressed in a power series of the length measured from the leading edge of the plate. Neglecting the heat conduction along the plate, Bryson and Edwards [4] obtained an exact solution for the problem. They used the Lighthill's approximate solution [5] to estimate the aerodynamic heating rate. The Lighthill solution does not involve any restriction on the wall-temperature distribution. It is applicable even when there exists a discontinuity in the temperature distribution. Since the temperature along the plate is hardly regarded as uniform, the heat conduction effect may not be neglected and it might be desirable to extend their solution to include the heat conduction in the plate. Kondo and Koyanagi [6] calculated the temperature distribution of a wedge in a supersonic flow, applying the Chapman and Rubesin solution.

The decrease of the strength of materials at higher temperatures is a problem of importance for the design of supersonic airplanes. Therefore we shall investigate the possibility of restriction of temperature rise by means of a jointed coating of materials with different melting point on the surface of the wing or the body.

## THE EQUATION OF HEAT TRANSFER IN A PLATE

A flat plate is placed parallel to a uniform flow, extending from $x = 0$, the leading edge, to $x = L$, the trailing edge, in the direction of the $x$-axis.

The equation describing the heat transfer in the plate is

$$C_m \rho_m h_m \frac{\partial T_w}{\partial t} = \lambda_m h_m \frac{\partial^2 I}{\partial x^2} + \dot{q}(t, x) \tag{1}$$

where we assume that the plate is so thin that the temperature gradient normal to the surface can be neglected. $C_m$, $\rho_m$, $h_m$, and $\lambda_m$ are the heat capacity, the density, the thickness, and the thermal conductivity of the

plate, respectively. The left-hand side of this equation represents the time rate of change in heat content and the first term on the right-hand side means the heat conduction, while the last term is the heat transferred per unit time from the boundary layer to a unit area of the plate.

The heat-transfer rate $\dot{q}(t,x)$, at point $x$ on the plate at time $t$ depends on the boundary-layer flow, and since the latter is determined by the temperature distribution on the plate $T_w(t,x)$ and the heat-transfer rate $\dot{q}$ depends not only on the temperature at that point but also on the temperature distribution over the whole plate, this means that $\dot{q}$ may be expressed as a functional of $T_w$—that is, we can write

$$\dot{q}(t,x) = F\left[T_w(t,\overset{L}{\underset{0}{x}})\right] \tag{2}$$

For the steady-state laminar boundary layer of a flat plate, Chapman and Rubesin [3] determined the heat-transfer rate as

$$F[T_w(x)] = \lambda_\infty \sqrt{\frac{u_\infty}{\nu}} \frac{1}{\sqrt{x}} \sum a_n y_n'(0) x^n \tag{3}$$

where $\lambda_\infty$, $\nu$ and $u_\infty$ are heat-conduction coefficient, kinematic viscosity, and the uniform velocity of the air respectively.

$a_n$ and $y_n'(0)$ are certain constants and Eq. (3) is restricted to the case where the surface temperature can be expressed in a power series of $x$ as

$$T_w(x) - T_\infty = n(0) + \sum_0^\infty a_n x^n y_n(0) \tag{4}$$

Lighthill [5] obtained an approximate expression

$$F[T_w(x)] = 0.332\lambda_\infty \sqrt{\frac{u_\infty}{\nu}} \Pr^{2/3} \frac{1}{\sqrt{x}} \int_0^x \frac{d[T_e - T_w]/d\xi}{(x^{3/4} - \xi^{3/4})^{1/3}}\, d\xi \tag{5}$$

In this expression, Pr stands for Prandtl number and $T_e$ for equilibrium temperature which is determined as

$$T_e = T_\infty + \Pr^{1/2} \frac{u_\infty^2}{2C_p} \tag{6}$$

where $C_p$ is the specific heat at constant pressure of air, $T_\infty$ is the temperature of the uniform flow. In the foregoing expressions, we notice that there exists a singularity of the type $x^{1/2}$ at the origin. This is caused by the fact

that the boundary layer is extremely thin at the leading edge. It is interesting to note that Eq. (3) depends on the temperature distribution on the whole plate while Lighthill's expression depends solely on the temperature between 0 and $x$ on the plate. In other words, the heat-transfer rate at a point depends, according to Lighthill, on the wall temperature in the upstream of the point and not on the overall temperature distribution. At any rate, Lighthill's expression can be applied to the case when discontinuities of the temperature distribution exist, as stated before.

In the present paper we apply the Lighthill formula and obtain an integro-differential equation for the wall temperature:

$$\frac{\partial T_w}{\partial t} = a_m^2 \frac{\partial^2 T_w}{\partial x^2} + 0.332 \sqrt{\frac{u_\infty}{\nu_\infty x}} \frac{\lambda_\infty \mathrm{Pr}^{1/3}}{C_m \rho_m h_m} \int_0^x \frac{d\,[T_e - T_w]}{\left[1 - \left(\frac{\xi}{x}\right)^{3/4}\right]^{1/3}} \tag{7}$$

where $a_m = \sqrt{\lambda_m / C_m \rho_m}$ is the thermal diffusibility.

Since Eq. (7) includes derivatives of $T_w(t,x)$ of the first order with respect to $t$, and of the second order with respect to $x$, we have to impose one initial condition and two boundary conditions to determine a particular solution of the equation. As the initial condition, we have

$$T_w(0,x) = T_\infty \tag{8}$$

On the other hand, since the heat inflow rate at the leading edge is infinite, we assume that the temperature there is always equal to the equilibrium temperature $T_e$. In determining the solution for ordinary heat-transfer problems, it is sufficient to assume, in addition, that the temperature should be kept finite all through the conducting body. However, for the present case, this weak condition is not enough to determine a solution. Emmons assumed that

$$\frac{\partial T_w}{\partial x} = 0 \qquad \text{at } x = 0 \text{ and } x = L$$

Since no heat source or sink exists at the trailing edge, let us put

$$\frac{\partial T_w}{\partial x} = 0 \qquad \text{at } x = L \tag{9}$$

as the other boundary condition. One can assume that the heat carried away in the wake is negligible. The assumption of Eq. (9) is confirmed by an experiment. We measured the temperature distribution over a steel

plate, placed parallel in a supersonic wind tunnel at Mach 2.4, finding that the temperature distribution is almost flat in the rear part of the plate (Fig. A).

Now since the equation is linear in $T_w$, we would like to find the indicial admittance of the system—that is, the transient temperature variation of the plate when it is suddenly placed into a uniform flow. In other words, we shall solve the equation by taking

$$u_\infty = u_\infty E(t)$$

where $E(t)$ is the Heaviside unit function.

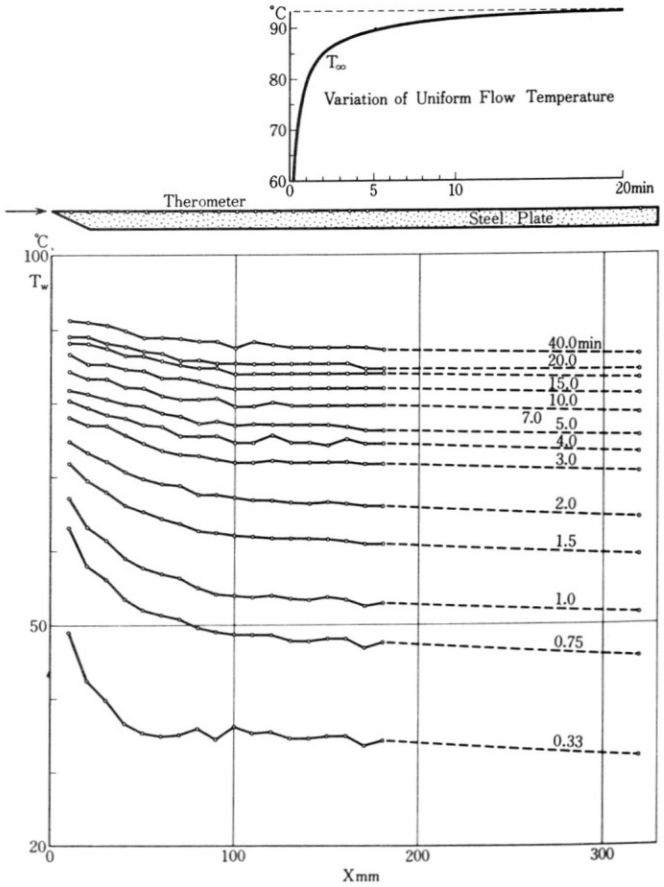


Figure A. Temperature distribution (steel plate, $L$ = 330 mm, $h$ = 10 mm, $M$ = 2.2).

Introducing nondimensional length and time as

$$\eta = \frac{x}{L}, \qquad \tau = \frac{a_m^2}{L^2} t$$

Eq. (7) is rewritten as

$$\frac{\partial T_w}{\partial \tau} = \frac{\partial^2 T_w}{\partial \eta^2} + B \frac{1}{\sqrt{\eta}} \int_0^\eta \frac{d[T_e - T_w]}{\left[1 - \left(\frac{\xi}{\eta}\right)^{3/4}\right]^{1/3}} \tag{10}$$

where

$$B = 0.332 \left(\frac{\lambda_\infty}{\lambda_m}\right) \mathrm{Pr}^{1/3} \sqrt{\frac{u_\infty L}{\nu_\infty}} \left(\frac{L}{h_0}\right)$$

and the initial and the boundary conditions are

$$\begin{aligned} T_w(0,\eta) &= T_\infty \\ T_w(\tau,0) &= T_e E(t) \end{aligned} \tag{11}$$

and

$$\left(\frac{\partial T_w}{\partial \eta}\right)_1 = 0$$

## SOME REMARKS ON NUMERICAL ANALYSIS

It is still hard to find the solution in a closed form, and therefore we resort to the numerical analysis, where steps in $\tau$ and $\eta$ are taken as $k$ and $h$, respectively; as

$$\Delta\tau = k \qquad \text{and} \qquad \Delta\eta = h \tag{12}$$

For a parabolic type equation, we should take

$$r \equiv \frac{k}{h^2} < \frac{1}{2} \tag{13}$$

Therefore, if we increase the number of points on the plate, we must take $\Delta\tau = k$ small and a long consecutive computation must be carried out before the equilibrium state is obtained. Numerical examples are worked out by taking $h = 0.2$ or $0.1$.

In a finite-difference form, Eq. (7) becomes

$$T_w(jh, \tau + k) = rT_w(\overline{j+1}\,h, \tau) + (1 - 2r)T_w(jh, \tau) + rT_w(\overline{j-1}\,h, \tau) + Bk \sum_{i=1}^{j} F(j, i)[T_0(ih, \tau) - T_0(\overline{i-1}\,h, \tau)]$$

$$(j = 1, 2, \ldots, n) \tag{14}$$

where we have

$$F_{ji} = \frac{1}{\sqrt{jh}} \frac{1}{h} \int_{(i-1)h}^{ih} \left[1 - \left(\frac{\xi}{jh}\right)^{3/4}\right]^{-1/3} d\xi \tag{15}$$

which is computed by Simpson's integral formula.

To carry out numerical example, the following values are assumed:

| | | |
|---|---|---|
| Mach number of the uniform flow | $M_\infty$ | = 2 |
| temperature of the uniform flow | $T_\infty$ | = 0 |
| thermal conductivity | $\lambda_\infty$ | = 0.240 kcal/mh deg |
| Prandtl number | Pr | = 0.71 |
| kinematic viscosity for air and | $\nu_\infty$ | = 0.154 cm²/sec |
| length | $L$ | = 1,000 mm |
| thickness for the dimensions of the plate | $h_m$ | = 1 mm |

**TABLE 1. NUMERICAL VALUES OF PARAMETERS**

| Metal | $\lambda_m$ | $a_m^2$ | $B$ | $a_m^2/\lambda_m$ | $k$ | $r$ | Equivalent time |
|---|---|---|---|---|---|---|---|
| Steel | 62 | 0.073 | 69.4 | 0.00118 | $10^{-3}$ | 1/40 | 0.822 |
| Duralumin | 141 | 0.240 | 32.5 | 0.0017– | $5 \times 10^{-2}$ | 1/20 | 0.500 |
| Copper | 332 | 0.404 | 12.9 | 0.00121 | $2 \times 10^{-2}$ | 1/8 | 0.742 |

## RESULTS AND DISCUSSIONS

The results of the numerical computations are shown in Figs. 2–8.

### NONSTEADY TEMPERATURE DISTRIBUTIONS

Figures 2–5 indicate the temperature distribution on steel, duralumin and copper plates.

## ACCURACY OF THE NUMERICAL ANALYSIS

In Fig. 2, the effect of the magnitude of steps in $\eta$ is indicated. The thick lines show the temperature distribution at various times when we take $\Delta\eta = 0.1$ or 10 points. The difference is large when $t$ is small in the neighbourhood of 20 percent chord while it is negligible after 10 minutes or in the rear part of the plate. We can infer that the exact solution may show a little lower temperature near the leading edge at earlier times. However,

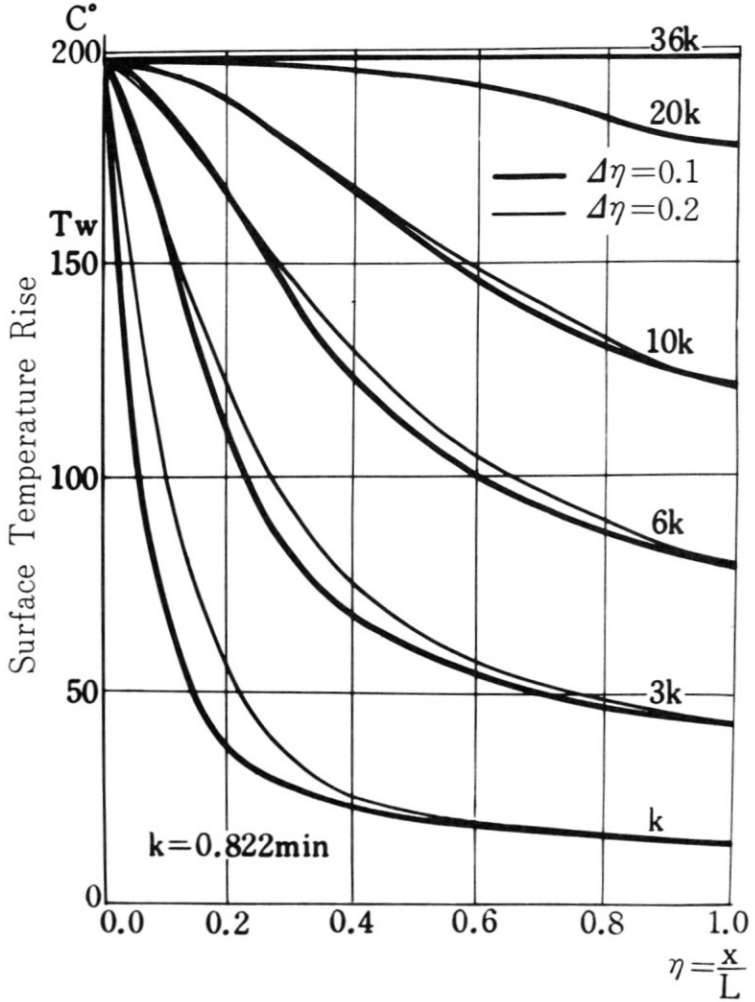


Figure 2. Temperature distribution (steel plate, $L$ = 1,000 mm, $h$ = 1 mm), $M_\infty = 2$, $T$ = 20°C.

since the temperature inclination is very steep, it recovers quite rapidly, while in the rear part of the plate the approximate solutions include smaller errors. We can also conclude that after about 10 minutes, the difference between the approximate and exact solutions are not perceptible.

## EFFECT OF HEAT CONDUCTION

In Fig. 4 the dotted lines indicate the solutions with the heat conduction in the plate neglected, which correspond to the Bryson-Edwards analysis.

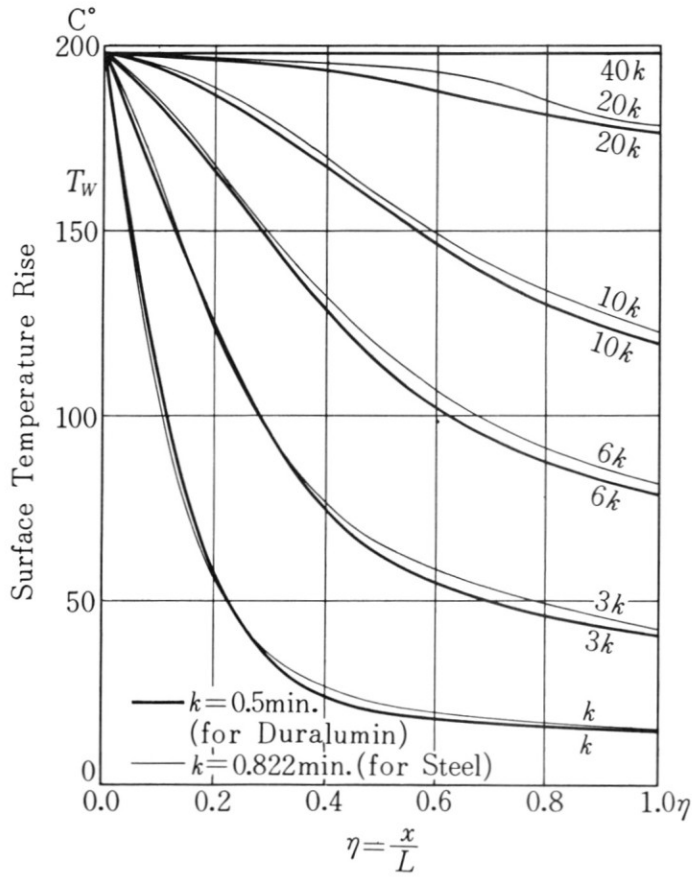


Figure 3. Temperature distribution (Duralumin plate, $L$ = 1,000 mm, $h$ = 1 mm), $M_\infty = 2$, $T$ = 20°C.

The temperature distributions are compared for the plate, for which the effect of heat conduction may be most evident.

If the heat conduction is neglected, the temperature near the stagnation point is shown to be much lower than the actual case in the earlier stage. On the other hand, the temperature close to the leading edge is reduced by conduction after some time, so that the solution with heat conduction neglected, indicates higher temperature at 7 minutes.

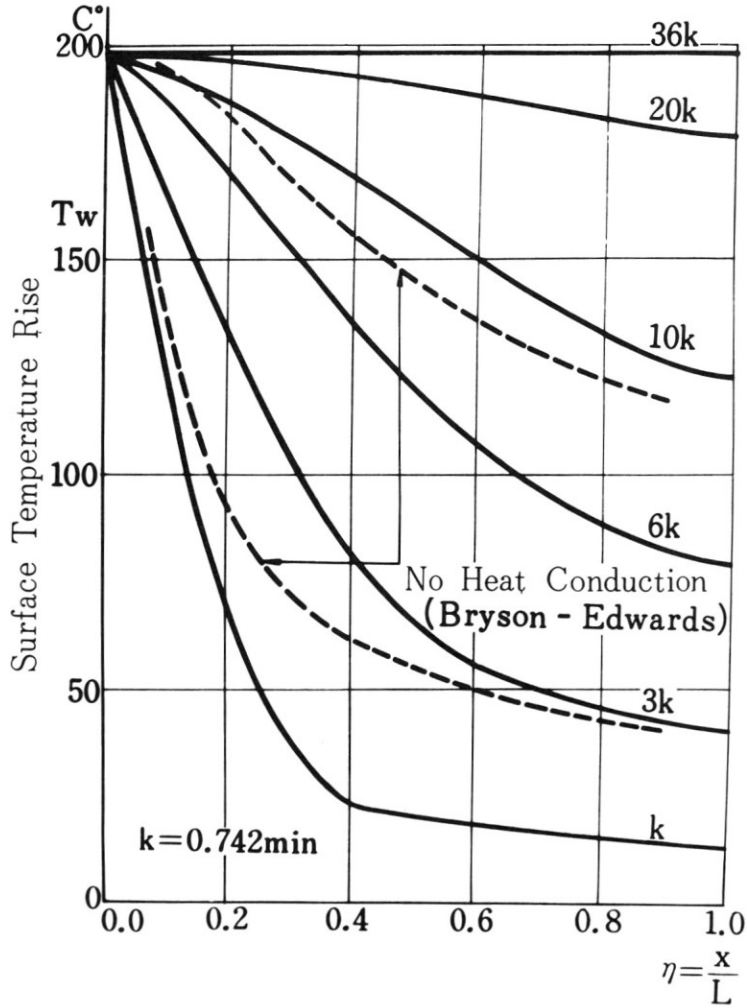


Figure 4. Temperature distribution (copper plate, $L$ = 1,000 mm, $h$ = 1 mm), $M_\infty = 2$, $T$ = 20°C.

## TEMPERATURE EQUILIBRIUM

The temperature rise by heat conduction is proportional to the second derivative of the temperature with respect to $x$, which approaches zero as the time elapses. The temperature of the plate is elevated mainly by the aerodynamic heating which is later represented in the last term of Eq. (7). Because $B$ is proportional to $a_m^2/\lambda_m = 1/C_m\rho_m$, Fig. 5 shows that the time required for the equilibrium state to be reached is in the order of magnitude of $B$ for various materials.

## TEMPERATURE DISTRIBUTION ON A JOINTED PLATE

A 500-mm long and 1-mm thick steel plate is jointed with a Duralumin plate of equal dimensions. The temperature distribution over this jointed plate in a uniform flow at Mach 2 is indicated in Fig. 6. The temperature rise in the part of Duralumin is rapid in the earlier stage. This high temperature is conducted on both sides and the curve becomes flat after several minutes.

The numerical solutions are carried out for this case in a similar way as stated above. The conditions at the jointed point are taken as

$$T_1(0.5, \tau) = T_2(0.5, \tau)$$

$$-\lambda_1 \left(\frac{\partial T_1}{\partial \eta}\right)_{0.5} = -\lambda_2 \left(\frac{\partial T_2}{\partial \eta}\right)_{0.5}$$

where $T_1$, $T_2$; $\lambda_1$ and $\lambda_2$ are the temperature and heat conductivity of each material.

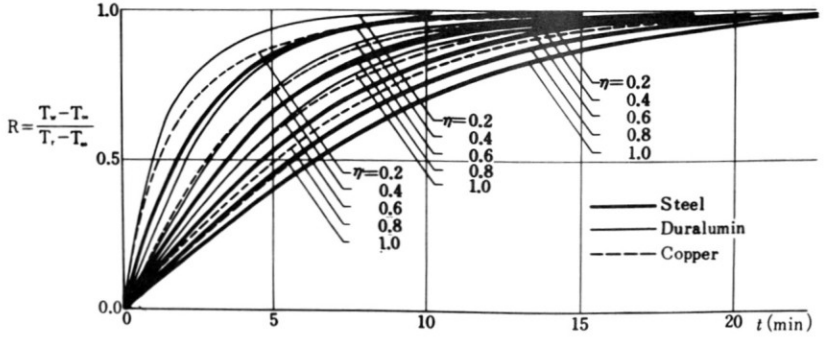


Figure 5. Temperature recovery at various points ($M_\infty = 2$, $L = 1{,}000$ mm, $h = 1$ mm).

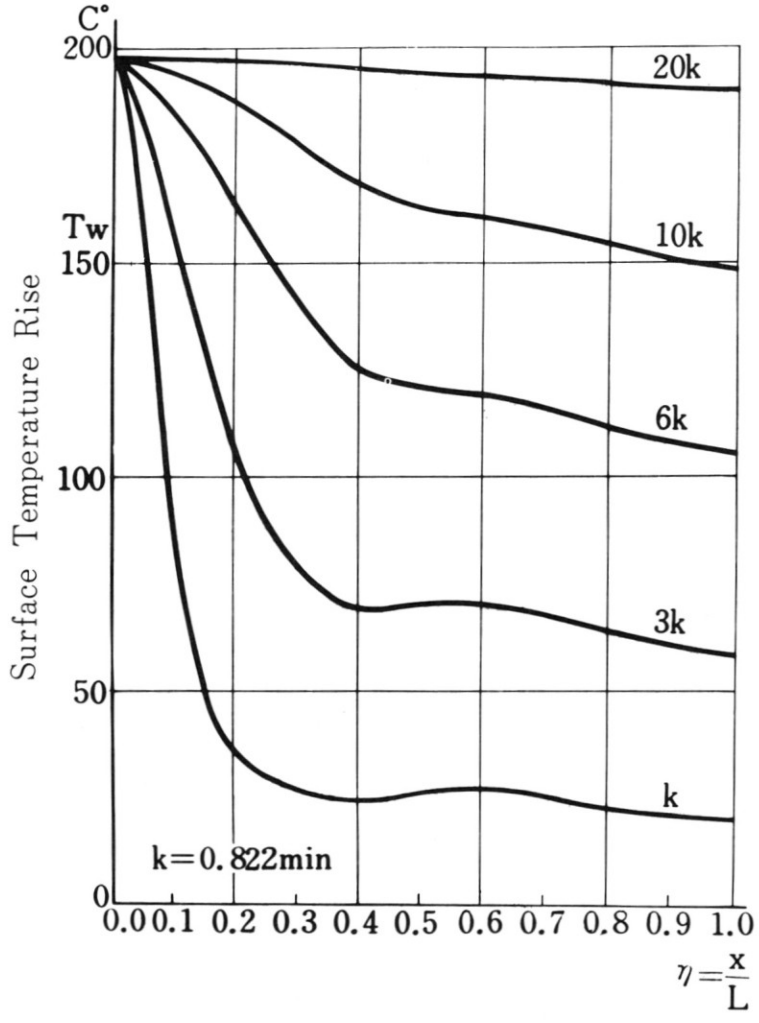


Figure 6. Temperature distribution (steel-Duralumin plate, $L$ = 1,000 mm, $h$ = 1 mm), $M_\infty = 2$, $T$ = 20°C.

## SIMILARITY PARAMETERS

The recovery factor is defined as

$$r = \frac{T_w - T_\infty}{T_e - T_\infty}$$

for the surface temperature $T_w$; see Eq. (10). Therefore the value of $B$ is the sole parameter to determine the recovery factor. That is

$$r(\tau) = f(B), \qquad \tau = \frac{(a_m{}^2)}{(L^2)t}$$

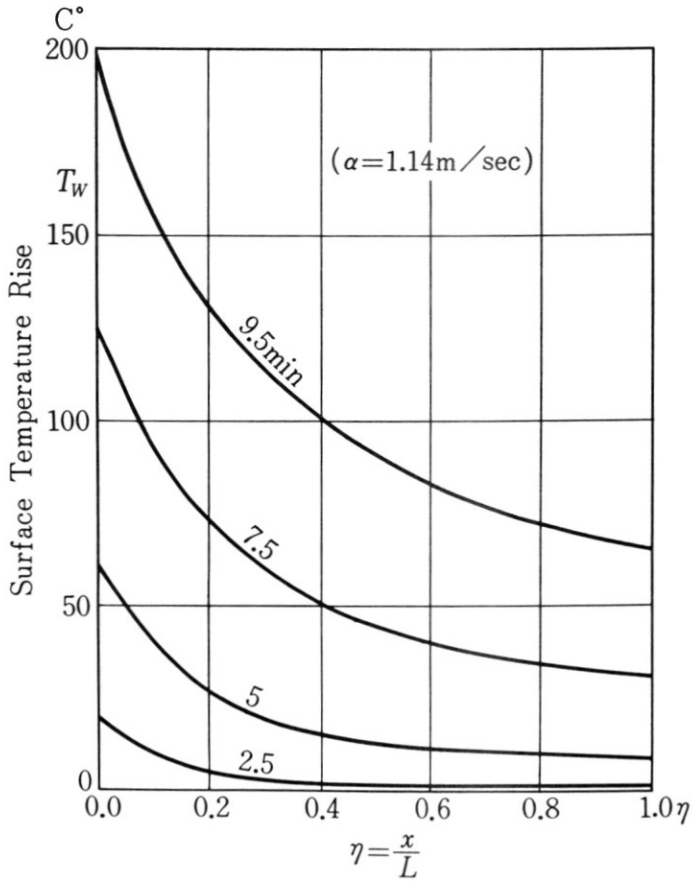


Figure 7. Temperature distribution of uniformly accelerated plate.

The effect of dimensions is represented by $L^{3/2}/h^{\circ}$ for recovery factor and $1/L^2$ for time.

## THICK PLATE

The temperature distributions on a steel plate of 10-mm thickness are worked out for the same condition. Figure 7 shows that the effect of the aerodynamic heating is much smaller than in the thin-plate case. Due to the larger heat capacity, the temperature rise is more gradual than in the case for a thin plate.

## ACCELERATED FLIGHT

Since the equation is linear and an initial temperature has been obtained, we can calculate the temperature variation for an arbitrary flight condition by simple superposition of the solutions. As an example, a case of uniformly accelerated motion is carried out.

$$\alpha = 1.14 \text{ m/sec}^2$$

The results are indicated in Fig. 8.

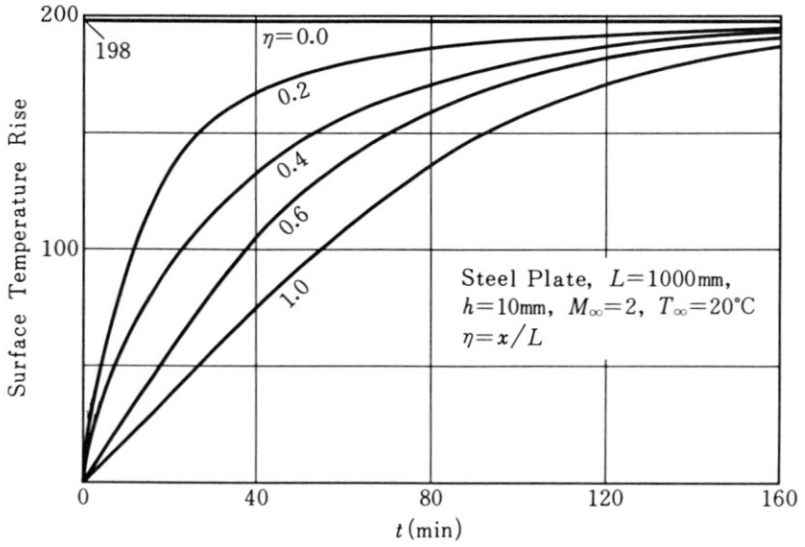


Figure 8. Surface temperature rise at various points.

## HYPERSONIC SPEED

The surface temperature variations of a thin steel plate of the same dimensions as treated before, at Mach 7 are shown in Fig. 9.

In this case, instead of Eq. (5), we used an expression like Eq. (3), taking into account the shock-boundary-layer interaction. The rear part of the plate will reach the equilibrium temperature in a shorter time, due to the large aerodynamic heating. However, the present writer hesitates to apply the result to practical situations since the equilibrium temperature is far beyond the melting point of steel.

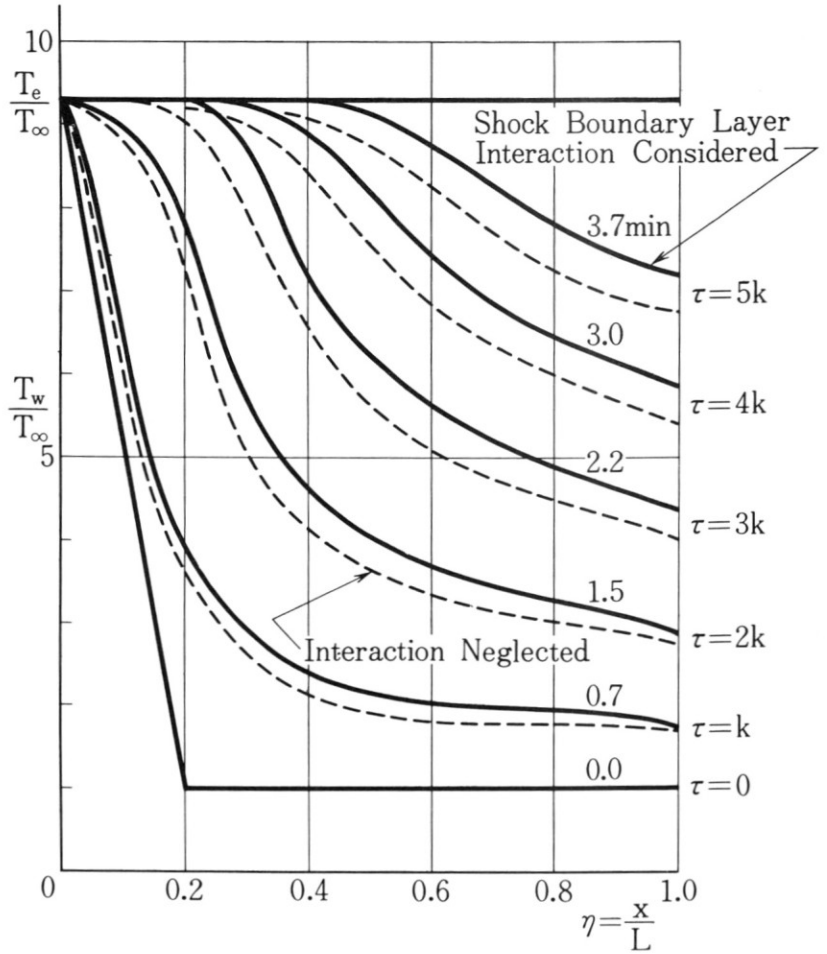


Figure 9. Temperature distribution (steel plate, $L$ = 1,000 mm, $h$ = 1 mm) $M_\infty$ = 7, $T_\infty$ = 216.5 °K = − 56.5°C.

## PART II

## INTRODUCTION

It is one of the most serious problems to find some means of reducing the tremendous amount of heat inflow to a space vehicle in the reentry stage. Water-film cooling, gas injection cooling and ablation seem to be most prospective countermeasures.

However, if there is a possibility of decreasing the amount of aerodynamic heating by changing the reentry path, it would be worthwhile to investigate the trajectory of that kind. When the vehicle has lifting surfaces, one can change the flight path by pilot control without any additional device.

The trajectory may be so determined as to restrict either the maximum heating rate at the stagnation point of the vehicle or the maximum acceleration during the reentry flight in the earth's atmosphere.

Here we shall define the optimum trajectory as the flight path among all admissible reentry paths along which the total amount of aerodynamics heat transfer will become minimum. The total heat transfer will be proportional to the amount of cooling materials consumed.

The heat-transfer rate $\dot{q}$ to some area of a vehicle depends on the velocity $v$, the density $\rho$ and the temperature $T$ of the atmosphere. The variation of $T$ between 100 km and 0 km altitudes is in a ratio of

$$10^{-1} \quad \text{to} \quad 1$$

whereas the corresponding variation of $\rho$ is

$$10^{-8} \quad \text{to} \quad 1$$

Therefore the effects on the heat transfer of the atmospheric-temperature variation can be neglected for the engineering practice.

We shall assume that

$$\dot{q} = K\rho^x v^y \tag{16}$$

where $K$ is a characteristic constant for the vehicle, and $x$ and $y$ are dimensionless positive exponents. The appropriate values of the exponents are

$$x = 1, \; y = 3$$

for the whole wetted surface,

$$x = \tfrac{1}{2}, \; y = 3$$

when the boundary layer is laminar, and

$$x = \tfrac{4}{5},\ y = 3 + \tfrac{4}{5}$$

when turbulent, for an area near the stagnation point of a blunt body [1].

The total heat inflow during the reentry flight is

$$Q = \int_0^T K\rho^x v^y\, dt \tag{17}$$

where $T$ is the total flight time from the initial altitude $Z = 0$ to the earth surface $Z = H$. Since we have

$$\frac{dZ}{dt} = v \sin \varphi \tag{18}$$

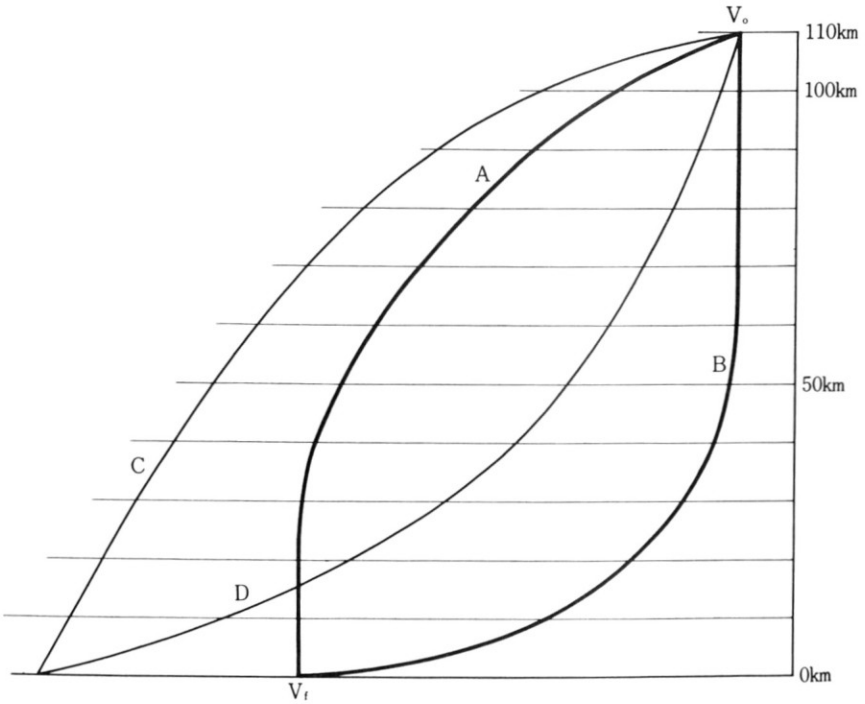


Figure 10. Various kinds of reentry paths.

where $\varphi$ is the flight-path angle measured with respect to the horizontal line, Eq. (17) is rewritten as

$$Q = \int_0^H \frac{K\rho^x v^{y-1}}{\sin \varphi} dZ \tag{19}$$

We can imagine several trajectories as drawn in Fig. 10. Along the path $A$ the vehicle comes down with a decreasing speed and then passes straight downwards through the dense atmosphere. Then the vehicle will experience a high rate of aerodynamic heating, but the period of aerodynamic heating will be short. Along the path $B$ the vehicle enters vertically into the rare atmosphere, reducing the heating time and then pulls up reducing the velocity in the dense air. The curves $C$ and $D$ are the modifications of $A$ and $B$. Along the path $C$ the vehicle will encounter a lower aerodynamic heating rate in a longer time compared to the path $D$. Thus it is hard to determine the optimum trajectory by a simple insight.

If the total loss of mechanical energy is to turn into the aerodynamic heat transfer from the boundary layer of the vehicle, then the optimum path would be the one which terminates at the maximum speed on the earth's surface.

Miele [2] studied the drag modulation program for minimizing the total heat input for a nonlifting reentry body.

## GENERAL CASE (LIFTING CASE)

Now we shall turn to the general case when the drag is related to the lift, so that

$$C_D = f(C_L) \tag{20}$$

The equations of motion of the vehicle are

$$\frac{\bar{w}}{g}\frac{dv}{dt} = \bar{w} \sin \varphi - \frac{1}{2}\rho v^2 S C_D$$

and

$$\frac{\bar{w}}{g}\frac{v^2}{r} = \bar{w} \cos \varphi - \frac{1}{2}\rho v^2 S C_L$$

where $r$ is the radius of curvature of the flight path. Since

$$\frac{v}{r} = \frac{d\varphi}{dt}$$

the equations reduce to

$$\frac{dv}{dZ} = \frac{g}{v} - \frac{1}{2}\frac{Sg}{w}\frac{\rho}{\sin\varphi} vf(C_L) \tag{21}$$

and

$$\frac{d\varphi}{dZ} = \frac{g}{v^2}\cot\varphi - \frac{1}{2}\frac{Sg}{w}\frac{\rho}{\sin\varphi} C_L \tag{22}$$

respectively, where $C_L$ must satisfy the following inequality:

$$C_{L_{\min}} \leqq C_L \leqq C_{L_{\max}} \tag{23}$$

The optimization problem is formulated as follows: in the class of functions: $C_L(z)$, $v(z)$, and $\varphi(z)$ which satisfy Eqs. (21), (22), and (23) with the prescribed initial values $C_L(0)$, $v(0)$, and $\varphi(0)$, find a particular combination of functions which extremizes the integral

$$Q = \int_0^H K\rho^x v^{y-1}/\sin\varphi \, dZ \tag{24}$$

The augmented function for this conditional variation principle is

$$\begin{aligned} F &= K\rho^x v^{y-1}/\sin\varphi \\ &+ \lambda_1\left\{\frac{dv}{dZ} - \frac{g}{v} + \frac{1}{2}A\frac{\rho}{\sin\varphi} vf(\eta)\right\} \\ &+ \lambda_2\left\{\frac{d\varphi}{dZ} - \frac{g}{v^2}\cot\varphi + \frac{1}{2}A\frac{\rho}{\sin\varphi}\eta\right\} \end{aligned} \tag{25}$$

where

$$A = \frac{Sg}{w} \qquad \text{and} \qquad \eta = C_L$$

The Euler-Lagrange equations are

$$\begin{aligned} &K(y-1)\rho^x v^{y-2}/\sin\varphi + \lambda_1\left\{\frac{g}{v^2} + \frac{1}{2}A\frac{\rho}{\sin\varphi} f(\eta)\right\} \\ &\quad + \lambda_2\left(\frac{2g}{v^3}\cot\varphi\right) - \frac{d\lambda_1}{dZ} = 0 \end{aligned} \tag{26}$$

$$\begin{aligned} &\left[K\rho^x v^{y-1} + \lambda_1\left\{\frac{1}{2}A\rho v f(\eta)\right\} + \lambda_2\left(\frac{1}{2}A\rho\eta\right)\right]\frac{\cos\varphi}{\sin^2\varphi} \\ &\quad - \lambda_2\frac{g}{v^2}\frac{1}{\sin^2\varphi} + \frac{d\lambda_2}{dZ} = 0 \end{aligned} \tag{27}$$

and

$$\lambda_1 v f'(\eta) + \lambda_2 = 0 \tag{28}$$

where

$$f'(\eta) = \frac{df}{d\eta}$$

The system of Eqs. (21), (22), (26), (27), and (28) and the inequality (23) furnish us with the fundamental equations to determine $\eta$, $v$, $\varphi$, $\lambda_1$, and $\lambda_2$.

## A SIMPLE CASE (NONLIFTING CASE)

Suppose a space vehicle has a configuration as illustrated in Fig. 11. Since it has a blunt nose, the change of the flow pattern around the body due to the variation of flow direction will be small. The lateral force to the

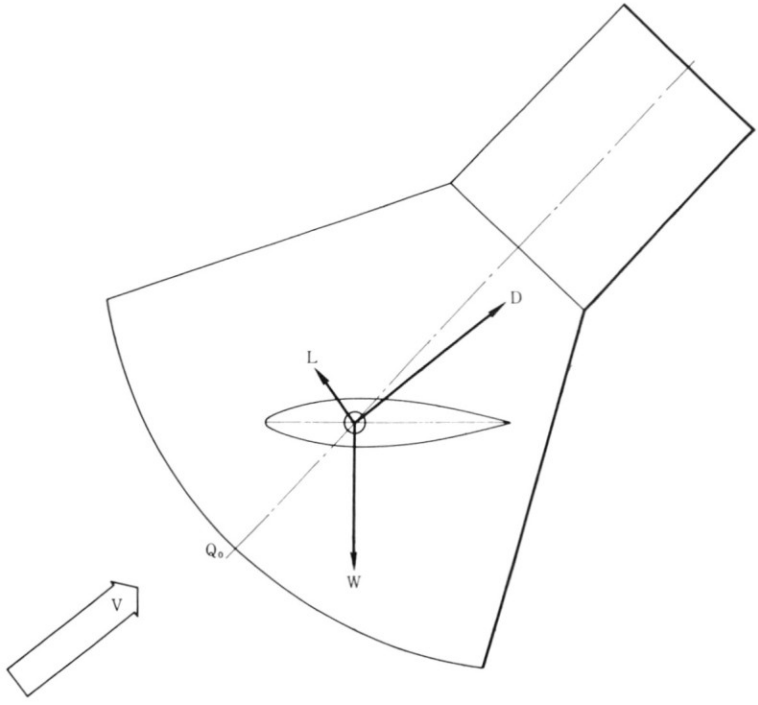


Figure 11. A winged reentry vehicle.

body being negligible, the total life is produced by the lifting surfaces or by some lifting facilities.

We shall take the drag coefficient as constant:

$$f(\eta) = C \tag{29}$$

Since

$$f'(\eta) = 0$$

we have

$$\lambda_2 = 0$$

by Eq. (28), and Eq. (27) yields

$$(K\rho^x v^{y-1} + \lambda_1 \tfrac{1}{2} AC\rho v) \frac{\cos \varphi}{\sin^2 \phi} = 0$$

Consequently, either

$$K\rho^x v^{y-1} + \lambda_1 \tfrac{1}{2} AC\rho v = 0 \tag{30}$$

or

$$\frac{\cos \varphi}{\sin^2 \varphi} = 0 \tag{31}$$

must hold. However, the transversality condition for the variation is

$$[\lambda_1 \delta v + \lambda_2 \delta \varphi]_0^H = 0$$

Consequently,

$$[\lambda_1]_{Z=H} = 0$$

must hold.

However, in general,

$$K\rho^x v^y$$

does not vanish at $Z = H$, and hence Eq. (30) will not hold.

Accordingly, we have

$$\varphi = \frac{\pi}{2} \tag{32}$$

from Eq. (31). This means that the vertical path is the optimum trajectory.

In this case, we have

$$C_L = 0 \tag{33}$$

by Eq. (22).

This case is not very interesting.

If we use the wing as a spoiler, we can modulate the drag by changing the angle. Then we have

$$C_{D\min} \leqq C_D \leqq C_{D\max} \tag{34}$$

We shall introduce a reduced vertical distance:

$$h = \int_0^Z \rho^x dZ \tag{35}$$

Then the total heat transfer is expressed as

$$Q = \int_0^I K v^y \, dh \tag{36}$$

where $I$ is the total reduced distance, that is

$$I = \int_0^H \rho^x \, dZ \tag{37}$$

Obviously, since a smaller velocity corresponds to a smaller transfer,

$$C_D = C_{D\max} \tag{38}$$

will give the minimum heat transfer.

If we impose a restriction on the total reentry time or on the terminal velocity of the vehicle, the optimum modulation programming for the minimum heat transfer will result in a more interesting case. Miele investigated such cases.

## THE NONEXISTENCE OF THE SOLUTION $\varphi = \pi/2$

In order to see that the general case includes a more interesting trajectory, we shall prove the nonexistence of the solution $\varphi = \pi/2$. If we suppose $\varphi = \pi/2$, then we have $\eta = 0$ or $C_L = 0$ from Eq. (18), and

$$f(\eta) = C, \quad f'(\eta) = E$$

The fundamental system becomes

$$\frac{dv}{dZ} = \frac{g}{v} - \frac{1}{2}AC\rho v \tag{39}$$

$$Ky\rho^x v^{y-1} + \lambda_1\left(\frac{g}{v^2} + \frac{1}{2}AC\rho\right) - \frac{d\lambda_1}{dZ} = 0 \tag{40}$$

$$-\lambda_2\frac{g}{v^2} + \frac{d\lambda_2}{dZ} = 0 \tag{41}$$

and

$$\lambda_1 Ev + \lambda_2 = 0 \tag{42}$$

From Eqs. (39), (41), and (42), we have

$$\frac{d\lambda_1}{dZ} = \frac{1}{2}\lambda_1 AC\rho \tag{43}$$

Therefore, Eq. (40) yields

$$Ky\rho^x v^{y-1} + \lambda_1\frac{g}{v^2} = 0$$

or

$$Ky\rho^x v^{y+1} + \lambda_1 g = 0 \tag{44}$$

Hence $\lambda_1$ must be negative.

On the other hand, we have

$$\lambda_1 = \exp\left\{\frac{1}{2}AC\int\rho\, dZ\right\} \tag{45}$$

from Eq. (43). Equation (45) implies that $\lambda_1$ is positive. Therefore, the solution for the general case does not include the vertical path $\varphi = \pi/2$.

## NUMERICAL EXAMPLES AND DISCUSSIONS

The variational problem with additional conditions can be solved numerically. Numerical examples have been carried out for the following sets of parameters:

$$K = 1, \quad H = 12 \times 10^4, \quad g = 9.8, \quad A = 9.8 \times 10^{-3}$$

$$v(0) = 10 \times 10^3, \quad \varphi(0) = 9°, 18°, 27°, \ldots, 90°;$$

$$C_L(0) = 1.0, 3.0$$

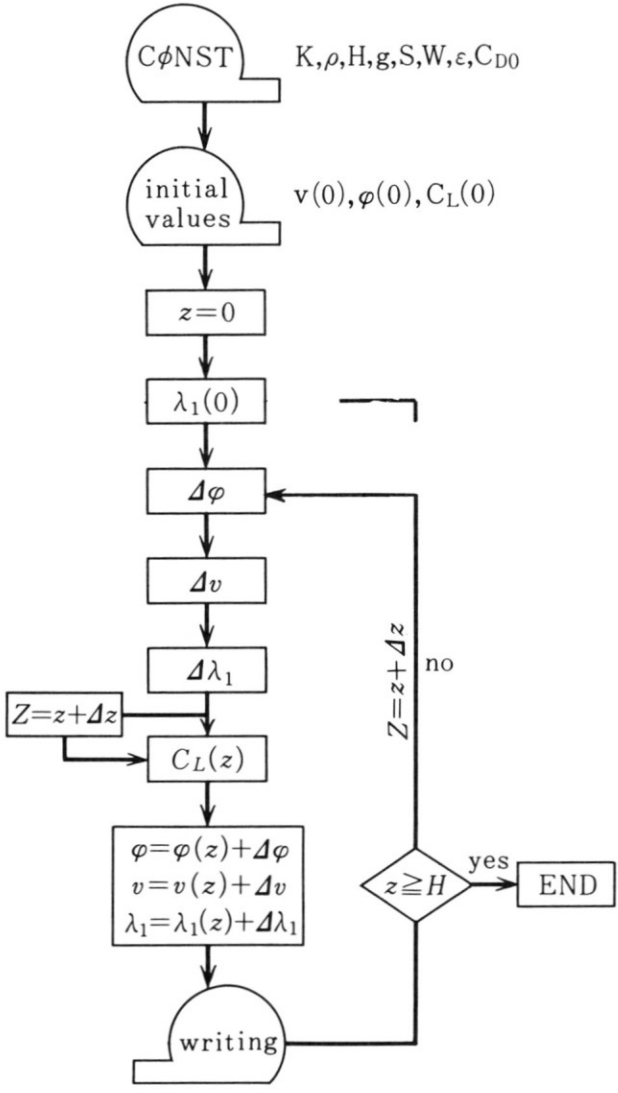


Figure 12. The flow chart for the computation.

The standard atmosphere table is used for $\rho(Z)$, the flow chart for the computation on an electronic computer is indicated in Fig. 12, where $\Delta Z = 1 \times 10^3$.

1. The optimum flight paths are shown in Figs. 13 and 14 in a vertical plane, where the shape of $f(\eta)$ is assumed as indicated in Fig. 13. In the upper atmosphere where the density of air is extremely low, the flight-path angle remains almost constant, while in the denser atmosphere the vehicle pulls up several times to reduce the velocity.
2. The variations of velocity as well as the heat-transfer rate per l-km vertical descent are indicated in Fig. 15. Although the velocities in the upper atmosphere are the same for the two cases, because of the longer flight time along the inclined path, the heat-transfer rate per unit distance of vertical descent becomes larger for the path. However, since the scale for the heat-transfer rate is logarithmic, the actual difference is not so large as would appear from the figure. We also notice that the curves coincide in the lower region. The optimum trajectory changes a great deal, depending on the initial incident angle, while the velocity variation and the heat-transfer rate are not very much influenced by the incident angle.

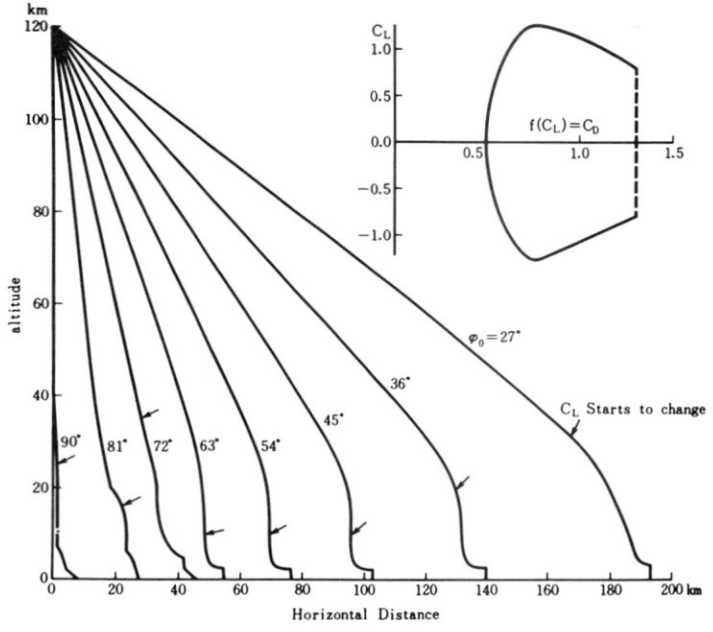


Figure 13. Optimum paths for various reentry angles (Laminar).

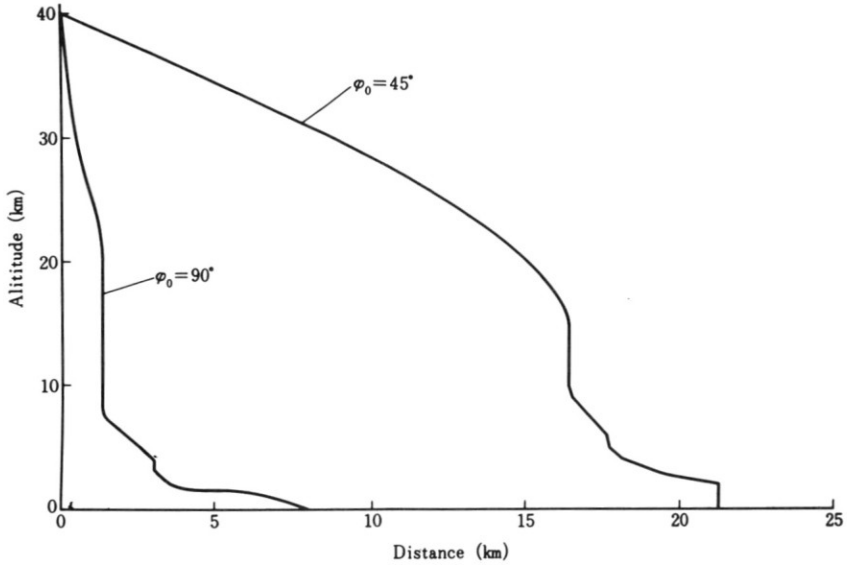


Figure 14. Optimum paths; details from Fig. 13 in the low-altitude region.

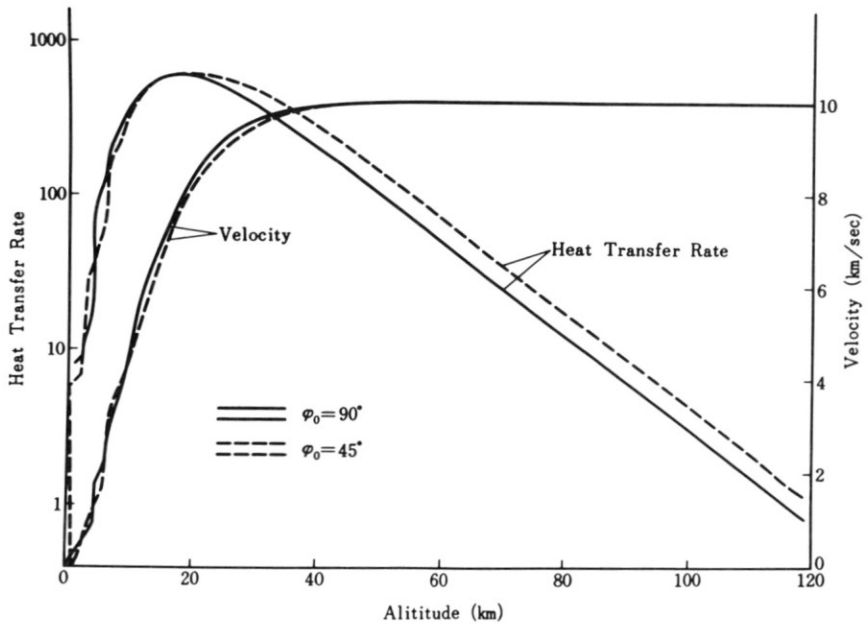


Figure 15. Variations of velocity and heat-transfer rate corresponding to Fig. 13.

3. In Fig. 16 are shown some interesting trajectories obtained for the cases of greater initial reentry angles. In this case the lift-drag relation is linear, as

$$f(\eta) = 1.00 + \eta$$

which might be the case for a diamond wing or a double wedge wing. The vehicle ascends for a while making use of the gravity com-

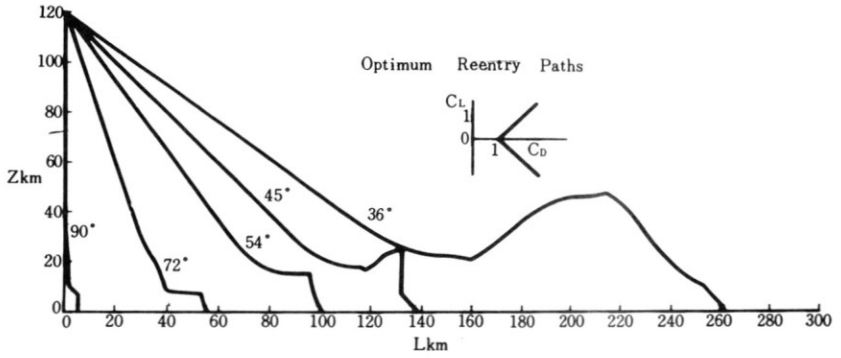


Figure 16. Optimum reentry paths for linear lift-drag relation.

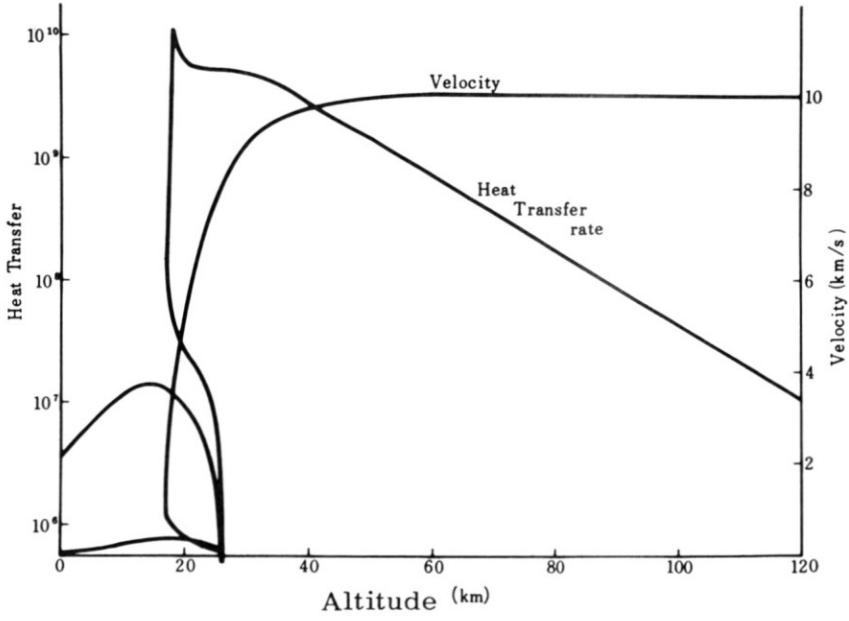


Figure 17. Variations of velocity and heat-transfer rate corresponding to Fig. 16.

ponent to reduce the velocity. The velocity and the heat-transfer rate are shown in Fig. 17.

4. In the present study we are interested in the laminar heat transfer at the stagnation point. However, the optimum problems for the turbulent heat transfer as well as the heat transfer on the whole wetted surface can be treated in a similar way. In Figs. 18 and 19 are shown corresponding results for a vehicle with $f(\eta)$ in Fig. 13.

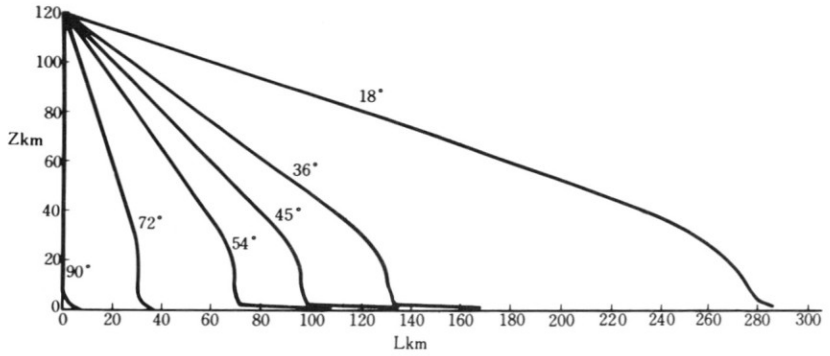


Figure 18. Optimum reentry paths (turbulent).

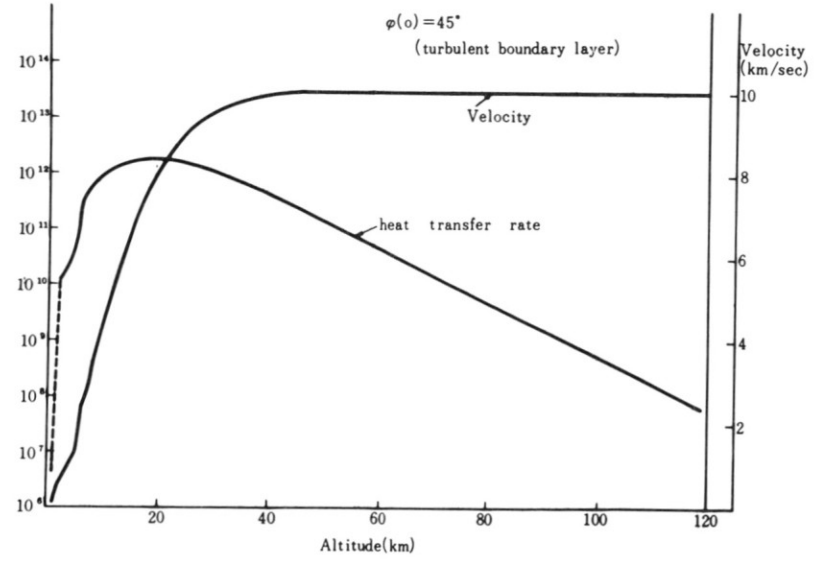


Figure 19. Variations of velocity and heat-transfer rate corresponding to Fig. 18.

## REFERENCES


### PART I

1. Kondo, J., "Survey of Aerodynamic Heating Problems," *J. Japan Soc. for Aero/Space Sci.*, vol. 6 (1958), pp. 72–81.
2. Moore, F. K., "Unsteady Laminar Boundary-Layer Flow," NACA TN 2471 (1951).
3. Chapman, D. R., and M. W. Rubesin, "Temperature and Velocity Profiles in the Compressible Laminar Boundary Layer with Arbitrary Distribution of Surface Temperature," *J. Aero. Sci.*, vol. 16 (1949), pp. 547–565.
4. Lighthill, M. J., "Contributions to the Theory of Heat Transfer through a Laminar Boundary Layer," *Proc. Roy. Soc.*, vol. *A*, 202 (1950), pp. 359–377.
5. Emmons, H. W., "The Non-Steady Aerodynamic Heating of a Plate," *50 Jahre Grenzschichtforschung* (1955), pp. 385–392.
6. Bryson, A. E., and R. H. Edwards, "The Effect of Non-Uniform Surface Temperature on the Transient Aerodynamic Heating of Thin-Skinned Bodies," *J. Aero. Sci.*, vol. 19 (1952), pp. 471–475.
7. Kondo, J., and Y. Koyanagi, "Aerodynamic Heating of Flat Wall," *Proc. 8th Japan Nat. Congr. Appl. Mech.* (1958), pp. 335–338.
8. Lo, H., "Determination of Transient Skin Temperature of Conical Bodies during Short Time High Speed Flight," NACA TN 1725 (1948).

### PART II

1. Truit, R. W., *Aerodynamic Heating* (New York: Ronald, 1960).
2. Miele, A., "The Calculus of Variations in Applied Aerodynamics and Flight Mechanics," in G. Leitmann (ed.), *Optimization Techniques* (New York: Academic, 1962).
3. Kondo, J., "Optimum Re-Entry Trajectory of Minimizing Aerodynamic Heating," *Proc. 5 ISTS*, Tokyo, 1963.


## COMMENTARY

K. L. C. LEGG (*Loughborough College of Technology, Loughborough, Leicester, England*): I should like to ask the author if he could provide some details of the wind-tunnel tests effected on the thin metal plates to corroborate the unsteady temperature distribution calculations. Such experimental work is extremely valuable as we tend to make many theoretical predictions on heat-transfer problems which can often be suspect due to dubious physical assumptions that have to be made and there is a great need to develop good experimental techniques to assist theoretical advance.

## REPLY

The experiments were carried out in a supersonic wind tunnel at the National Aero/Space Laboratory in Tokyo. Besides it took some time to establish a steady flow in the tunnel; the stagnation temperature changed gradually as shown in Fig. A, and we could not compare the data with the theory. We only verified the appropriateness of the assumption $\partial T/\partial x = 0$ at the trailing edge.

## COMMENTARY

DR. A. VAN DER NEUT (*Technical University, Delft, Netherlands*): The assumption was made that the boundary condition at the trailing edge is $\partial T/\partial x = 0$. It is true for the blunt trailing edge where the heat transfer through the blunt edge will be negligibly small. However, with sharp trailing edges $\partial T/\partial x$ will not vanish. My question is: What was the shape of the trailing edge of the plates, which showed when tested that $\partial T/\partial x$ could be assumed to be zero?

## REPLY

The trailing edge of the plate was actually blunt as shown in Fig. A. However, the limiting case when the thickness of the plate can be neglected is being considered, and therefore the assumption of the shape of the trailing edge will have little influence on the results.

## COMMENTARY

JOHN JELLINEK (*Johns Hopkins University, Applied Physics Laboratory, Silver Spring, Maryland*): Have you considered nonequilibrium dissociated air effects in your reentry studies? These may considerably affect the heat input to leading edges of a vehicle on a sharp reentry trajectory.

## REPLY

No. However, the effects of nonequilibrium dissociated air, when properly described mathematically, can be introduced into the equation presented in the paper, and then solutions for optimum reentry maneuver, corresponding to minimum total heat input, can be obtained.